Extending the Higgs Boson Reach at the Upgraded Fermilab Tevatron

Tao Han and Ren-Jie Zhang
Department of Physics, University of Wisconsin, 1150 University Avenue, Madison, Wisconsin 53706
(Received 21 July 1998)

We study the observability of a standard-model-like Higgs boson at the upgraded Fermilab Tevatron via the modes $p\overline{p} \to gg \to h \to W^*W^* \to \ell\nu jj$ and $\ell\overline{\nu}\ell\nu$. We find that, with c.m. energy of 2 TeV and an integrated luminosity of 30 fb^{-1}, the signal may be observable for the mass range of $135 \lesssim m_h \lesssim 180$ GeV at a $(3-5)\sigma$ statistical level. We conclude that the upgraded Fermilab Tevatron may have the potential to detect a standard-model-like Higgs boson in the mass range from the CERN e^+e^- collider LEP II reach to 180 GeV. [S0031-9007(98)08153-8]

PACS numbers: 14.80.Bn, 13.85.Qk

The Higgs bosons are crucial ingredients in the standard model (SM) and its supersymmetric (SUSY) extensions. Searching for Higgs bosons has been one of the major motivations in the current and future collider programs since they most faithfully characterize the mechanism for the electroweak gauge symmetry breaking. Experiments at the e^+e^- collider LEP II will eventually be able to discover a SM-like Higgs boson with a mass about 105 GeV [1]. The CERN Large Hadron Collider (LHC) should be able to cover the full range of theoretical interest, up to about 1000 GeV [2].

It has been discussed extensively how much the Fermilab Tevatron can do for the Higgs boson search. It appears that the most promising processes continuously going beyond the LEP II reach would be the electroweak gauge Higgs boson associated production [3–5] $p\overline{p} \to Wh, Zh$. The leptonic decays of W, Z provide a good trigger, and $h \to b\overline{b}$ may be reconstructible with adequate b tagging. It is now generally believed that for an upgraded Fermilab Tevatron, with c.m. energy $\sqrt{s} = 2$ TeV and an integrated luminosity $\mathcal{O}(10-30)$ fb^{-1}, a SM-like Higgs boson can be observed up to a mass of about 120 GeV [6]. The Higgs discovery through these channels crucially depends on the b-tagging efficiency and the $b\overline{b}$ mass resolution. It is also limited by statistics for $m_h > 120$ GeV. It may be possible to extend the mass reach to about 130 GeV and slightly beyond [5]. On the other hand, from the theoretical point of view, weakly coupled supersymmetric models generally predict the lightest Higgs boson to have a mass $m_h \lesssim 150$ GeV [7]. It would be of the greatest theoretical significance for the upgraded Fermilab Tevatron to extend the Higgs boson coverage over this range.

It is important to note that the leading production mechanism for a SM-like Higgs boson at the Fermilab Tevatron is the gluon-fusion process via heavy quark triangle loops. Although the decay mode $h \to b\overline{b}$ in this case would be swamped by the QCD background, the $h \to W^*W^*$ mode (where W^* generically denotes a W boson of either on- or off-mass shell) will have an increasingly large branching fraction for $m_h \gtrsim 130$ GeV and may have a chance to be observable. In this paper, we study in detail the observability of a SM-like Higgs boson at an upgraded Fermilab Tevatron for the modes

$$p\overline{p} \to gg \to h \to W^*W^* \to \ell\nu jj \quad \text{and} \quad \ell\overline{\nu}\ell\nu, \tag{1}$$

where $\ell = e, \mu$, and j is a light quark jet. In Fig. 1, we show the cross section for $gg \to h$ versus m_h with $p\overline{p}$ c.m. energy $\sqrt{s} = 2$ TeV. Along with the inclusive total cross section (solid curve), we show the W^*W^* (dashes) and Z^*Z^* (dots) channels, as well as their various decay modes $W^*W^* \to \ell\nu jj, \ell\overline{\nu}\ell\nu$ and $Z^*Z^* \to \ell\overline{\ell}\nu\overline{\nu}, 4\ell$. (We have normalized our signal cross section to include next-to-leading order QCD corrections [8], and we use the CTEQ4M distribution functions [9].) The scale on the right-hand side gives the number of events expected for 30 fb^{-1}. We see that, for the m_h range of current interest, there may be about 1000 events produced for $W^*W^* \to \ell\nu jj$ and about 100 events for $W^*W^* \to \ell\overline{\nu}\ell\nu$. This latter channel has been studied at the Superconducting Super Collider and LHC energies [10] and at a 4 TeV Fermilab Tevatron [4]. We find that at $\sqrt{s} = 2$ TeV, after nontrivial optimization for the signal identification for Eq. (1) over the substantial

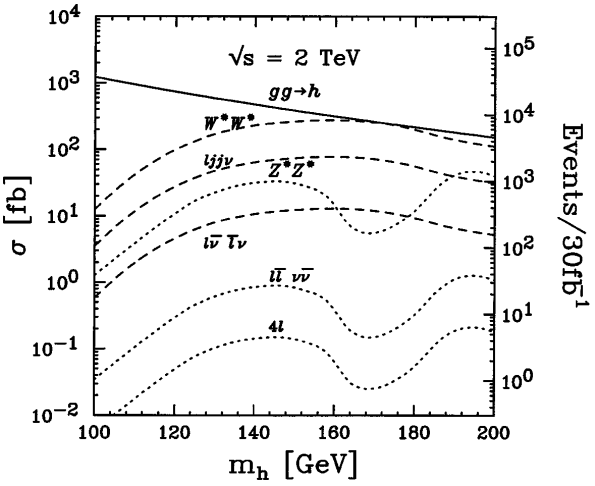

FIG. 1. The Higgs boson production cross section via the gluon-fusion process versus m_h at the 2 TeV Fermilab Tevatron. The $h \to W^*W^*$ (dashed lines) and Z^*Z^* (dotted lines) channels and various subsequent decay modes are also depicted.

SM backgrounds, it is promising to extend the Higgs boson reach at the upgraded Fermilab Tevatron with an integrated luminosity of 30 fb^{-1} to $m_h \approx 135$–180 GeV at a $(3-5)\sigma$ statistically significant level.

$W^*W^* \to \ell\nu jj$.—For this mode, we require the final state to have an isolated charged lepton (ℓ), large missing transverse energy ($\not{E}_T$), and two hard jets. The leading SM backgrounds are

$$\begin{aligned} &p\bar{p} \to W + 2 \text{ QCD jets}, \qquad p\bar{p} \to WW \to \ell\nu jj, \\ &p\bar{p} \to WZ(\gamma^*) \to \ell\nu jj, \qquad p\bar{p} \to t\bar{t} \to \ell\nu jjb\bar{b}. \end{aligned} \tag{2}$$

The background processes are calculated with the full SM matrix elements at tree level.

To roughly simulate the detector effects, we use the following energy smearing:

$$\begin{aligned} \Delta E_j/E_j &= 0.8/\sqrt{E_j} \oplus 0.05 \quad \text{for jets}, \\ \Delta E_\ell/E_\ell &= 0.3/\sqrt{E_\ell} \oplus 0.01 \quad \text{for leptons}, \end{aligned} \tag{3}$$

where $\oplus$ denotes a sum in quadrature. The basic acceptance cuts used here are

$$\begin{aligned} &p_{T\ell} > 15 \text{ GeV}, \qquad |\eta_\ell| < 1.1; \\ &p_{Tj} > 15 \text{ GeV}, \qquad |\eta_j| < 3; \\ &\not{E}_T > 15 \text{ GeV}; \qquad \Delta R(\ell j) > 0.3, \qquad \Delta R(jj) > 0.7. \end{aligned} \tag{4}$$

For the sake of illustration, we present our study mostly for $m_h = 140$ and 160 GeV, and we will generalize the results to the full m_h range of interest. The cut efficiency for the signal is about 35% (60%) for $m_h \approx$ 140 (160) GeV.

Since there are only two jets naturally appearing in the signal events, the $t\bar{t}$ background can be effectively suppressed by rejecting events with extra hard jets. We therefore impose

$$\text{Jet veto} \quad p_{Tj} > 15 \text{ GeV} \quad \text{in } |\eta_j| < 3. \tag{5}$$

The QCD background in (2) has the largest rate. The dijet in the signal is from a W decay, while that in the QCD background tends to be soft and collinear. We thus impose the cuts on the dijet:

$$\begin{aligned} &65 < m(jj) < 95 \text{ GeV}, \qquad \phi(jj) > 140^\circ; \\ &70 < m(jj) < 90 \text{ GeV}, \qquad \phi(jj) > 160^\circ, \end{aligned} \tag{6}$$

for $m_h = 140$ and 160 GeV, respectively, where $m(jj)$ is the invariant mass of the dijet, and $\phi(jj)$ is the opening angle of the two jets in the transverse plane. For $m_h \geq 160$ GeV, the $m(jj)$ distribution has a unique peak because both W bosons are on shell, so the $m(jj)$ cuts in Eq. (6) would not significantly harm the signal. On the other hand, for $m_h \leq 160$ GeV, nearly half of the signal will be cut off by the $m(jj)$ cuts, making this region of the Higgs mass more difficult to explore from this mode.

We have also examined other mass variables, such as the W-boson transverse mass $M_T(W)$, dijet-lepton invariant mass $m(jj\ell)$, and the cluster transverse mass M_C, which are defined as

$$\begin{aligned} M_T(W) &= \sqrt{(p_{T\ell} + \not{E}_T)^2 - (\vec{p}_{T\ell} + \vec{\not{p}}_T)^2}, \\ M_C &= \sqrt{p_T^2(jj\ell) + m^2(jj\ell)} + \not{E}_T. \end{aligned} \tag{7}$$

The $M_T(W)$ develops a peak near M_W for on-shell W decay. An upper cut on this variable below M_W can help remove the background from real W decay as long as m_h is less than 160 GeV. The cluster transverse mass M_C would be the most characteristic variable for the signal. It peaks near m_h and yields a rather sharp end point above m_h. To further improve the signal-to-background ratio S/B, we find the following tighter cuts helpful:

$$\begin{aligned} &100 < m(jj\ell) < 120 \text{ GeV}, \qquad \not{E}_T < 30 \text{ GeV}, \qquad 120 < M_C < 140 \text{ GeV}, \\ &35 < M_T(W) < 55 \text{ GeV}, \qquad 2.4 < \Delta R(jj) < 3.5; \\ &100 < m(jj\ell) < 130 \text{ GeV}, \qquad \not{E}_T < 50 \text{ GeV}, \qquad 130 < M_C < 170 \text{ GeV}, \\ &40 < M_T(W) < 90 \text{ GeV}, \qquad 2.8 < \Delta R(jj) < 3.5, \end{aligned} \tag{8}$$

for $m_h = 140$ and 160 GeV, respectively.

We show the results progressively at different stages of the kinematical cuts in Table I. We see that, for an integrated luminosity of 30 fb^{-1}, the signal for $m_h =$ 140 GeV is very weak while that for $m_h \sim 160$ GeV can reach a 3σ statistical significance.

$W^*W^* \to \ell\bar{\nu}\bar{\ell}\nu$.—For the pure leptonic channel, we identify the final state signal as two isolated charged leptons and large missing transverse energy. The leading SM background processes are

$$\begin{aligned} &p\bar{p} \to W^+W^- \to \ell\bar{\nu}\bar{\ell}\nu, \qquad p\bar{p} \to ZZ(\gamma^*) \to \nu\bar{\nu}\ell\bar{\ell}, \\ &p\bar{p} \to t\bar{t} \to \ell\bar{\nu}\bar{\ell}\nu b\bar{b}, \\ &p\bar{p} \to Z(\gamma^*) \to \tau^+\tau^- \to \ell\bar{\nu}\bar{\ell}\nu\nu_\tau\bar{\nu}_\tau. \end{aligned} \tag{9}$$

We first impose basic acceptance cuts

$$\begin{aligned} &p_{T\ell} > 10 \text{ GeV}, \qquad |\eta_\ell| < 1.1; \\ &p_{T\ell'} > 5 \text{ GeV}, \qquad |\eta_{\ell'}| < 2.5; \\ &m(\ell\ell') > 10 \text{ GeV}, \qquad \not{E}_T > 25 \text{ GeV}. \end{aligned} \tag{10}$$

The cut efficiency for the signal is about 70%. We also smear the lepton momenta according to Eq. (3), and veto the hard central jets via Eq. (5) to effectively remove the $t\bar{t}$ background. At this level, the largest background comes from the Drell-Yan process for $\tau^+\tau^-$ production. However, this background can be essentially eliminated by removing the back-to-back lepton pair events by requiring

$$\phi(\ell\ell) < 150^\circ. \tag{11}$$

TABLE I. $h \to W^*W^* \to \ell\nu jj$ signal and background cross sections (in fb) for $m_h = 140$ and 160 GeV, after different stages of kinematical cuts. A jet-veto cut in Eq. (5) has been implemented for the $t\bar{t}$ background.

σ [fb]	Basic cuts in (4)		Cuts in (6)		Cuts in (8)	
m_h [GeV]	140	160	140	160	140	160
Signal	23	49	8.8	21	2.2	15
Background						
Wjj	6.5×10^5		6.1×10^3	2.1×10^3	1.4×10^2	5.5×10^2
WW	1.3×10^3		5.5×10^2	2.4×10^2	17	55
WZ	66		20	7.0	0.3	1.3
$t\bar{t}$	0.4		0.1		0.0	
S/B	...		0.1%	0.9%	1.4%	2.5%
$S/\sqrt{B}$ (30 fb^{-1})	...		0.6	2.4	1.0	3.3

The W^*W^* mass cannot be accurately reconstructed due to the two undetectable neutrinos. However, both the transverse mass M_T and the cluster transverse mass M_C, defined as

$$M_T = 2\sqrt{p_T^2(\ell\ell) + m^2(\ell\ell)}\,, \qquad M_C = \sqrt{p_T^2(\ell\ell) + m^2(\ell\ell)} + \not{E}_T\,, \tag{12}$$

yield a broad peak near m_h. We note that these transverse mass variables are very important for the signal identification and for controlling the systematic error.

In Fig. 2(a), we show the M_C distributions for the $\ell\bar{\nu}\bar{\ell}\nu$ signal with $m_h = 140$, 160, and 180 GeV along with the leading backgrounds after the cuts in (10) and (11). Although the mass peaks in M_C are hopeful for signal identification, they are rather broad. We may have to rely on the knowledge of the SM background distribution. We hope that, with the rather large statistics of the data sample, one may obtain a good fit for the normalization of the background shape outside the signal region in Fig. 2(a), so that the deviation from the predicted background can be identified as signal. Some additional useful cuts are

$$m(\ell\ell) < 80 \text{ GeV} \qquad (70 \text{ for } m_h \le 140 \text{ GeV})\,, \qquad \not{E}_T < m_h/2, \qquad m_h/2 < M_C < m_h\,. \tag{13}$$

The results at different stages of kinematical cuts are shown in Table II. Because of the absence of the large QCD background in (2), this pure leptonic mode seems to be statistically more promising than the $\ell\nu jj$ mode. One may expect a more than 3σ (4σ) effect for $m_h = 140$ (160) GeV with 30 fb^{-1}. It was pointed out in [11] that some angular variables implement the information for decay lepton spin correlations and are powerful in discriminating against the backgrounds. With some further selective cuts on the angular distributions, we find that the S/B can be improved to about 8% and 21%, with the signal rates 2.6 and 3.3 fb for $m_h = 140$ and 160 GeV, respectively. We show in Fig. 2(b) the event rate distributions for the SM background (solid) and signal plus background (dashes) for $m_h = 160$ GeV. The statistical error bars on the background are also indicated.

In Fig. 3, we show the integrated luminosities needed to reach 3σ and 5σ significance versus m_h. The dotted curves are for the $\ell\nu jj$ mode and the dashed for $\ell\bar{\nu}\bar{\ell}\nu$. We consider that these two modes have rather different systematic errors, so that we can combine the results for them quadratically. This is shown by the solid curves. We see that, with an integrated luminosity of 30 fb^{-1}, one may be able to reach at least a 3σ signal for $135 \lesssim m_h \lesssim 180$ GeV. Taking into account the previous studies [3,5,6], we conclude that the upgraded Fermilab Tevatron with $\sqrt{s} = 2$ TeV and 30 fb^{-1} may have the potential to detect the SM-like Higgs boson in the mass range from the LEP II reach to 180 GeV. On the other hand, if there is only about 10 fb^{-1} data available, the sensitivity to the Higgs boson search via the modes of Eq. (1) would be very limited. A higher luminosity is strongly called for in this regard.

Finally, a few remarks are in order. (a) In our analyses, we have not considered the $W \to \tau\nu_\tau$ mode. Including this decay channel would increase the signal rate by a factor of 3/2 (9/4) for the $\ell\nu jj$ ($\ell\bar{\nu}\bar{\ell}\nu$) mode. But the signal identification would be more challenging. The other modes such as $Z^*Z^* \to \ell\bar{\ell}jj, \ell\bar{\ell}\nu\bar{\nu}$ and 4ℓ,

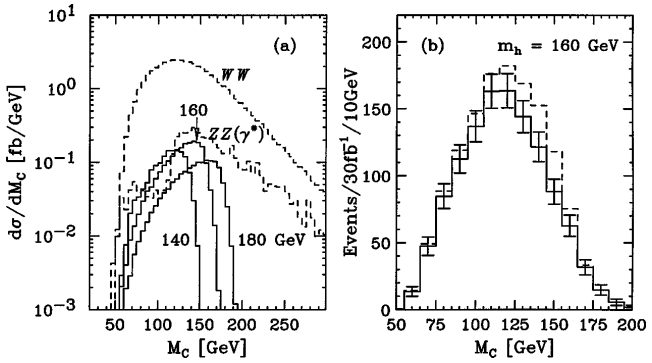

FIG. 2. The cluster transverse mass distributions for $\ell\bar{\nu}\bar{\ell}\nu$ mode (a) for the signal $m_h = 140$, 160, and 180 GeV and the leading SM backgrounds with cuts (10) and (11). With further selective cuts, we show the event rates in (b) for SM background (solid lines) and background plus signal (dashed lines) for $m_h = 160$ GeV. The statistical error bars are also indicated on the background curve in (b).

TABLE II. $h \to W^*W^* \to \ell\bar{\nu}\bar{\ell}\nu$ signal and background cross sections in (fb) for $m_h = 140$ and 160 GeV, after different stages of kinematical cuts. The last column corresponds to the refinement of mass cuts and various angular distribution cuts. A jet-veto cut in Eq. (5) has been implemented for the $t\bar{t}$ background.

σ [fb]	Basic cuts in (10)		$\phi(\ell\ell) < 150°$		Cuts in (13)		Refined cuts	
m_h [GeV]	140	160	140	160	140	160	140	160
Signal	7.3	10	7.0	9.9	6.3	9.1	2.6	3.3
Background								
WW	2.7×10^2		2.4×10^2		1.1×10^2	1.4×10^2	32	16
$ZZ(\gamma^*)$	24		18		1.8	1.8	0.3	0.1
$Z(\gamma^*)$	3.9×10^2		0.0		0.0		0.0	
$t\bar{t}$	0.2		0.1		0.0		0.0	
S/B	1.1%	1.5%	2.7%	3.9%	5.6%	6.4%	8.0%	21%
$S/\sqrt{B}$ (30 fb^{-1})	1.5	2.1	2.4	3.4	3.3	4.2	2.5	4.5

although smaller, may also be helpful to improve the signal observability. (b) Our results presented here are valid not only for the SM Higgs boson, but also for SM-like ones such as the lightest Higgs boson in SUSY at the decoupling limit. If there is an enhancement from new physics for $\Gamma(h \to gg) \times B(h \to WW, ZZ)$ over the SM expectation, the signal of Eq. (1) would be more viable. If $B(h \to b\bar{b})$ is suppressed, such as in certain parameter regions in SUSY, then the signal under discussion may complement the Wh, Zh $(h \to b\bar{b})$ channels at a lower m_h region.

Our results summarized in Fig. 3 based on the parton-level simulation are clearly encouraging to significantly extend the reach for the Higgs boson search at the upgraded Fermilab Tevatron. The more comprehensive results with full Monte Carlo simulations in a realistic environment will be reported elsewhere [12].

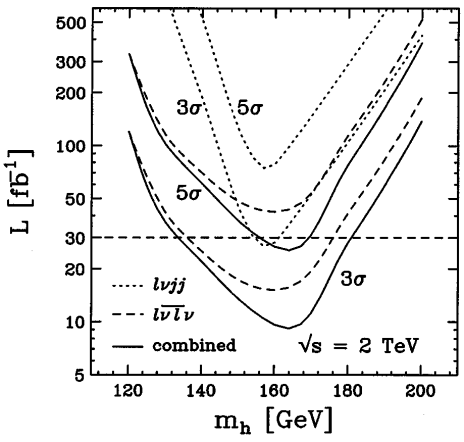

FIG. 3. The integrated luminosity needed to reach 3σ and 5σ statistical significance versus m_h. The dotted and dashed lines correspond to the $\ell\nu jj$ and $\ell\bar{\nu}\bar{\ell}\nu$ modes, respectively. The solid lines are the (quadratically) combined results.

We thank V. Barger, E. Berger, R. Demina, M. Drees, T. Kamon, S. Mrenna, J.-M. Qian, S. Willenbrock, and J. Womersley for helpful comments. T. H. thanks the Aspen Center for Physics for its hospitality during the final stage of the project. This work was supported in part by a DOE Grant No. DE-FG02-95ER40896 and in part by the Wisconsin Alumni Research Foundation.

[1] For a recent review on Higgs boson physics at LEP II, see, e.g., M. Carena *et al.*, in *Physics at LEP II*, CERN-96-01 (CERN, Geneva, 1996), p. 351.
[2] CMS Technical Design Report, CERN-LHCC-94-38; ATLAS Technical Design Report, CERN-LHCC-94-43.
[3] A. Strange, W. Marciano, and S. Willenbrock, Phys. Rev. D **49**, 1354 (1994); Phys. Rev. D **50**, 4491 (1994).
[4] J. Gunion and T. Han, Phys. Rev. D **51**, 1051 (1995).
[5] S. Mrenna and G. L. Kane, hep-ph/9406337; W. M. Yao, in *Proceedings of the Supersymmetry/Higgs Summary Meeting, Batavia, IL, 1998* (unpublished).
[6] S. Kim, S. Kuhlmann, and W. M. Yao, *New Directions for High-Energy Physics, Proceedings of the 1996 DPF/DPB Summer Study, Snowmass, CO, 1996* (Stanford Linear Accelerator Center, Menlo Park, CA, 1997), p. 610; W. M. Yao, *New Directions for High-Energy Physics, Proceedings of the 1996 DPF/DPB Summer Study, Snowmass, CO, 1996* (Stanford Linear Accelerator Center, Menlo Park, CA, 1997), p. 619.
[7] G. L. Kane, C. Kolda, and J. D. Wells, Phys. Rev. Lett. **70**, 2686 (1993).
[8] D. Graudenz, M. Spira, and P. M. Zerwas, Phys. Rev. Lett. **70**, 1372 (1993); M. Spira, A. Djouadi, D. Graudenz, and P. M. Zerwas, Nucl. Phys. **B453**, 17 (1995).
[9] CTEQ Collaboration, H. L. Lai *et al.*, Phys. Rev. D **55**, 1280 (1997).
[10] E. W. N. Glover, J. Ohnemus, and S. S. D. Willenbrock, Phys. Rev. D **37**, 3193 (1988); V. Barger, G. Bhattacharya, T. Han, and B. A. Kniehl, Phys. Rev. D **43**, 779 (1991).
[11] M. Dittmar and H. Dreiner, Phys. Rev. D **55**, 167 (1997).
[12] T. Han, A. Turcot, and R.-J. Zhang (to be published).